PROCEEDINGS of the
23rd International Congress on Acoustics

9 to 13 September 2019 in Aachen, Germany

Design of resonant vacuum pressure sensor with CMUT for high sensitivity and linearity

Xiaoli ZHANG[1]; Lu YU[1]; Haixia YU[1]; Dachao LI[1]

[1] Tianjin University, China

ABSTRACT

Vacuum pressure monitoring is mainly used for atmospheric pressure measurement and pressure measurement inside organisms, and is widely used in aviation, meteorology and medical diagnosis. This paper innovatively reports a vacuum pressure monitoring method using capacitive micromachined ultrasonic transducer (CMUT) array which is a small MEMS device manufactured by wafer bonding process. Both of the manufacturing process and detection circuits are simplified compared with those of the traditional MEMS devices used for vacuum pressure monitoring. By detecting the change of resonant frequency rather than capacitance of the CMUT array with varying vacuum pressure, the anti-interference ability of vacuum pressure(less than 1atm) monitoring is improved. Simulation and experimental results are consistent and show that the resonant frequency of the designed CMUT varies linearly with the applied pressure ranging from 20-101kPa. The sensor achieves high detection sensitivity of 438Hz/kPa and R-Square of 0.99335 at DC bias of 30V.

Keywords: CMUT, Resonant vacuum pressure sensor, DC bias

1. INTRODUCTION

Vacuum pressure sensors have been extensively utilized in modern aerospace field. Owing to the unique advantages of micro-electromechanical processing technology, MEMS pressure sensors are popular nowadays and mainly classified into silicon piezoresistive, silicon capacitive and silicon resonant pressure sensors (1). For all these sensors, technical indicators such as sensitivity, linearity, and detection range should be carefully considered.

Silicon piezoresistive pressure sensors ususally consist of pressure-sensitive resistor made on the pressure sensitive diaphragm. The pressure value is obtained by detecting change of the resistance. The merits like feasible preparation, convenient detection and low cost make it well developed. But for the problems such as zero and temperature drift, they are only generally suitable for the occasions with low requirements on accuracy and long-term stability (2). In general, there exists a trade-off between sensitivity and linearity (3). Silicon capacitive pressure sensors detect the capacitance change between the upper and lower electrodes of the sensor for the purpose of pressure detection. However, the sensitivity of capacitive pressure sensors is limited by compressive strain and high Young's modulus of the solid dielectric elastomer layers (4). Although some methods has been used to increase the sensitivity, the sensitivity decreases rapidly as the applied pressure increases and the fabrication process is complicated (5).

Silicon resonant pressure sensor, which measures external pressure by detecting the change of resonant frequency, is a typical representative of high precision pressure sensors. Organically combining mechanical resonance sensing technology and micro-electromechanical processing technology, silicon resonant pressure sensor not only has the advantages of high precision, good stability and quasi-digital output of traditional mechanical resonance sensor, but also has the characteristics of small volume, low power consumption, compatibility with integrated circuit technology, and easy to mass production (6-12).

The most common silicon resonant pressure sensor has composite structure of pressure sensitive diaphragm and resonator, in which the resonator is fixed on the surface of pressure sensitive diaphragm. The resonator is vacuum packaged and not easily affected by the external environment. However, the common complicated stress-relieving vacuum packaging, process and electrical feedthroughs to the outside make its design and fabrication a challenging problem, hindering its widespread application (13).

[1] zhangxl@tju.edu.cn

Z Li. et al (14) also used CMUT for ultra-low pressure measurement. They show that the resonant frequency of the CMUT varies linearly with the applied pressure, and the membranes of the biased CMUTs can produce a larger resonant frequency shift than the diaphragms with no DC bias. But they did not conduct experiments to demonstrate it.

In this paper, a CMUT array is firstly proposed for detection of high vacuum pressure and the tendency of frequency response is quite opposite from that in ultra-low pressure scope. Firstly, the influence of DC voltage and external pressure on the resonant frequency of CMUT was analyzed theoretically. Then finite element model was established to conduct modal analysis of the CMUT cell to determine the structure parameters. The vacuum bonding process was used to fabricate the CMUT device. Finally, an experimental system was built to carry out the pressure detection experiments of the CMUT device. High detection sensitivity of 438Hz/kPa and R-Square of 0.99335 are obtained in the pressure range of 20-101kPa. The pressure detection range can be easily changed by changing the structural parameters of CMUT. Therefore, CMUT devices have broad application prospects in the field of pressure detection.

2. Design

2.1 Design of CMUT Array

In this paper, a CMUT array composed of three elements was built for pressure detection, as shown in Figure 1. The array is designed on the basis of linear relationship between the resonant frequency and the external pressure. All the cells in each element are connected in parallel. The outer two elements were designed to validate the consistency of the process.

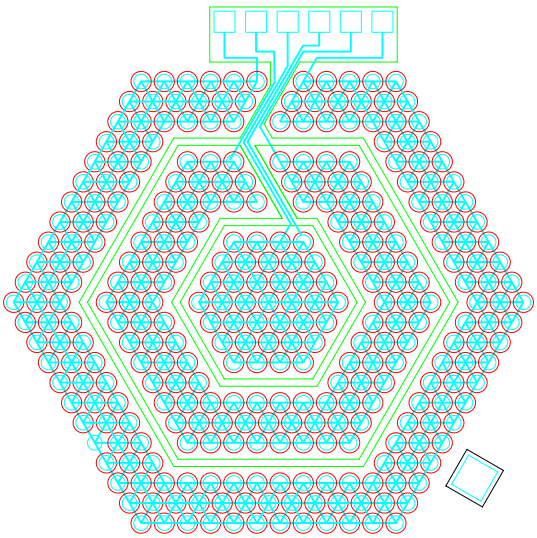

Figure 1 – CMUT array designed for pressure detection

Each cell in Fig.1 is composed of a metalized silicon membrane and fixed bottom electrode as well as the vacuum cavity between them, which is similar to a capacitor, as shown in Fig.2. When a DC bias voltage is applied to the top and bottom electrodes, the clamped flexible membrane is deformed towards the fixed bottom electrode to reach equilibrium. When an alternating current voltage is added, a periodic vibration of the membrane is obtained. The circular membrane is used in this paper for it greatly reduces stress concentration.

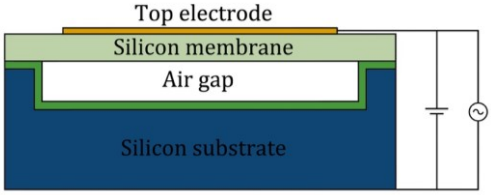

Figure 2 – Geometry of the CMUT cell

2.2 Theory Analysis of Structure Design

The variation of external pressure can lead to a resonant frequency shift of the vibrating membrane when the electrostatically actuated membranes are used as pressure sensors. As the pressure increases and the deflection-to-thickness ratio is higher than 0.2, the derived expressions in (15) are not valid. Therefore, the effect of electrostatic force and pressure on the resonant frequency of CMUT membrane needs to be reconsidered.

The "soft spring effect" that the resonant frequency of the vibrating membrane decreases with the increase of DC bias which is lower than collapse voltage has been widely studied and confirmed (16).

However, the resonant frequency of the CMUT membrane increases gradually as the external pressure gets higher, showing stress hardening effect or "hard spring effect".

It is interesting that hard spring effect and soft spring effect have opposite effect on the resonance frequency. The combined influence of these two factors is furtherly researched using the FEM model in the next section. In high pressure range, the former effect plays a leading role by reasonably design the structural parameters.

2.3 Simulation of CMUT Parameters

To understand the behavior of CMUT, a finite element model (FEM) was created in COMSOL Multiphysics (COMSOL, Inc., Burlington, MA, USA) to represent a circular CMUT cell. The model couples an electromechanics subdomain to the vacuum cavity and solid materials. The membrane layer (Si) is fixed at the edges to prevent translation motion but allow for deflection, and the insulation layer is SiO_2 (17).

Due to the limitation of the material, the thickness of CMUT membrane is set as 10μm. The insulation layer, which isolates the conductive silicon substrate from the top electrode, is set to be 2um to avoid shorting. In this paper, we proposed two structures for simulation. The dimensions of the two structures as well as the mechanical and electrical properties (density: ρ, Young's modulus: E, and Poisson's ratio: ν, relative permittivity, ε_γ) of the materials used in the FEM are listed in Table 1. The simulation results of structure 1 and 2 for pressure detection ranging from 20kPa to 101kPa are shown in Fig. 3 and 4, respectively.

Table 1 – Dimensions and properties of materials used in COMSOL model

	Structure 1 radius/thickness, μm	Structure 2 radius/thickness, μm	ρ, kg/m^3	E, GPa	ν	ε_γ
Top electrode	250/0.2	350/0.2	19300	70	0.44	--
Membrane	400/10	480/10	2329	130	0.18	11.7
gap	400/5	480/10	--	--	--	1
Insulation	400/2	480/2	2200	70	0.17	4.2

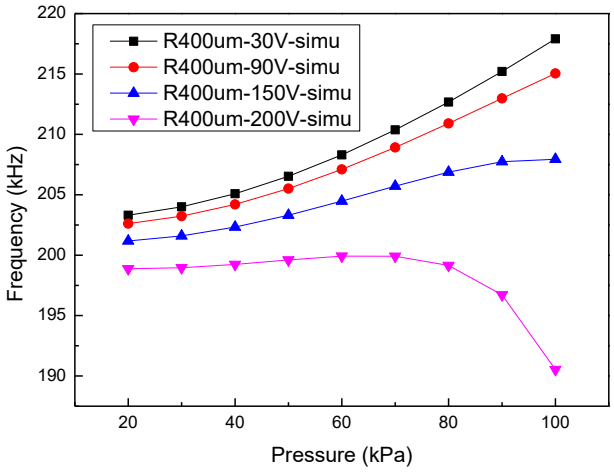

Figure 3 – The simulation results of structure 1 (R400μm, gap 5μm) for detection of 20-101kPa

It can be expected that in both figures, at given pressure, the resonant frequency falls down as the voltage increases because of the soft spring effect. In figure 3, the linearity of the curves gets worse with the increase of DC bias because the soft spring effect gets more effective. However, in figure 4, the variation of resonant frequency is not obvious as the DC bias gets larger for the spring softening effect is surmounted by the stress hardening effect which plays a leading role in changing the resonant frequency of the membrane. The resonant frequency increases linearly with the rise of pressure at a given DC bias voltage for structure 2 which is selected for the following fabrication and experiments.

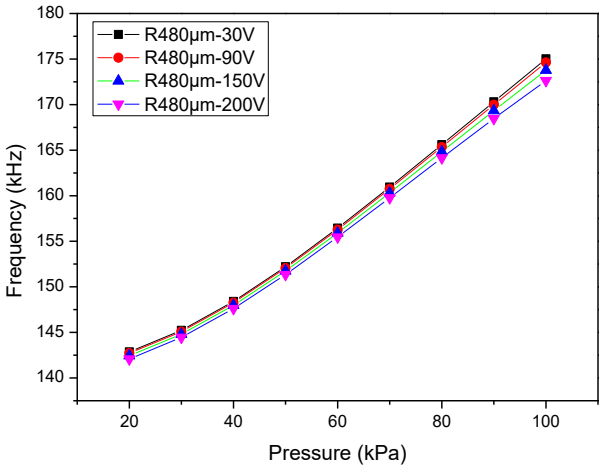

Figure 4 – The simulation results of structure 2 (R480μm, gap 10μm) for detection of 20-101kPa

3. Fabrication

The CMUT array was fabricated using Si wafer bonding process which introduces small stress, and good cell uniformity (18). It begins with two wafers: a prime quality silicon wafer and a SOI wafer. In its simplest form, the wafer-bonded CMUT process can be summarized as follows: The prime quality silicon wafer is thermally oxidized to a predetermined thickness (Fig. 5a), followed by a photolithography step to define the cavity shape (Fig. 5b). The silicon dioxide layer is dry etched through the photoresist pattern all the way to the silicon, as shown in Fig. 5c. After the photoresist is removed, another layer of silicon dioxide is thermally grown to form the insulation layer for isolating the conductive silicon substrate from the top electrode to avoid shorting (Fig. 5d). Following RCA cleaning and surface activated, the SOI wafer and the prime wafer are brought together in vacuum (Fig. 5e). After bonding and annealing, the handle of the SOI wafer as well as the buried oxide layer is removed to release the membranes (Fig. 5f). Openings through the silicon and silicon dioxide layers are defined with photolithography and etched through to access the bottom silicon layer and make the ground connection (Fig. 5g). Finally the top Au electrode was sputtered on the membranes to make the top connection (Fig. 5h). The elements are electrically isolated by etching all the way to the oxide layer. Wafer bonding process simplifies the process, reduces the number of steps and the turn-around time, eliminates problems with membrane release, high stress, and porous films, and increases the yield, uniformity, and process control.

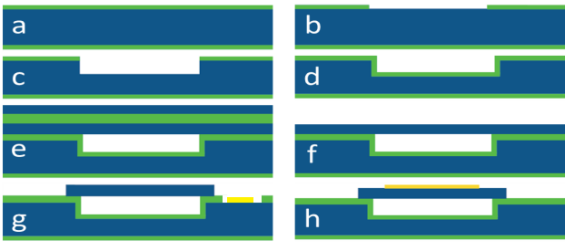

Figure 5 – Detailed view of the manufacture process of the CMUT array

The finished bare CMUT chip is glued on a specially designed printed circuit board (PCB), and the top and bottom electrodes of the CMUT device are wire bonded to the corresponding pads on PCB, as shown in Fig. 6a, the partial enlarged detail of the CMUT array is shown in Fig.6b. The gold color represents the gold electrode on the membrane. A cross-section view of a single cell of the CMUT array is shown in Fig.6c.

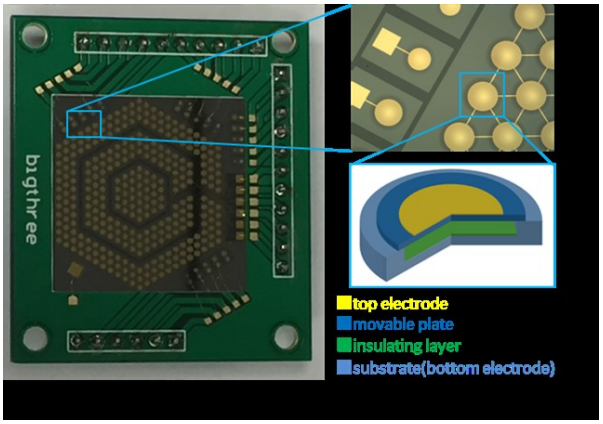

Figure 6 – (a) The photo of the CMUT array, (b) partial enlarged detail of the CMUT array, (c) a cross-section view of the CMUT cell.

4. Experiments

4.1 Pressure Detection System

After the top and bottom electrodes of the CMUT device are wire bonded to the corresponding pads on the PCB, a vacuum pressure detection system was built to perform measurements at elevated pressure. Figure 7 shows the schematic view of the experimental setup.

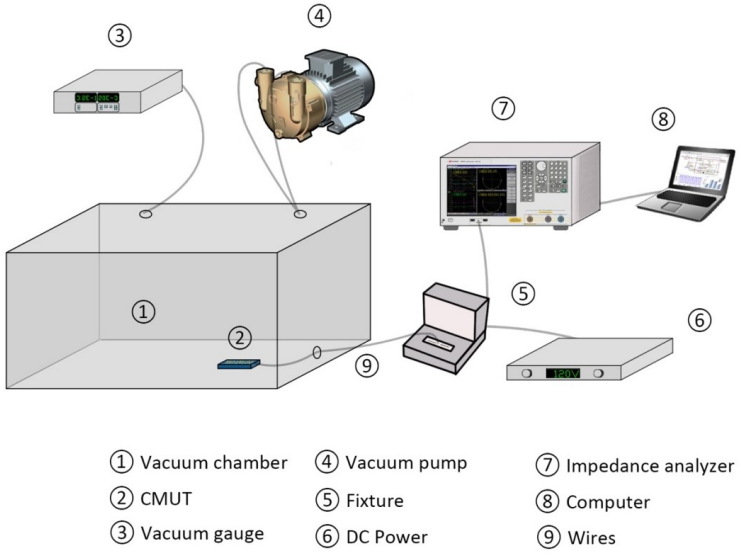

Figure 7 – Schematic view of the experimental setup

During the experiment, a vacuum pump is used to extract air from the chamber to provide vacuum pressure. The wires are inserted into the chamber through a plug. One ends of the wires are connected to the top and bottom electrodes of the CMUT device placed in the vacuum chamber, and the other ends are connected to the two ports of the impedance analyzer fixture. The output of DC source is connected to the impedance analyzer fixture which provides DC bias voltage to CMUT. At each DC bias, measurements were conducted by the impedance analyzer HP 4294 (Agilent Technolgies Inc., Palo Alto, CA, USA) to obtain electrical impedance curves of the CMUT device at various pressures. The measured data and curves can be recorded by the personal computer connected to the impedance analyzer.

4.2 Experiment Results and Discussion

The measured resonant frequency curves of the fabricated CMUT array are shown in Fig. 8. The linear fit was conducted for each curve at DC biases of 30V, 90V, 150V, 200V, respectively. Then the results were summarized in Table 2. High sensitivity and linearity were achieved, and the sensitivity at 30V can reach as high as 438Hz/kPa. According to the R-Square value of the curves under different DC biases, the

improvement of linearity is not obvious when the DC bias is increased from 30V to 200V. So 30V is preferred since low voltage is more convenient and safe. The experimental curve shows a good agreement with the FEM result as shown in Fig. 9. The FEM underestimates the magnitude of the resonant frequency for the internal stress of the CMUT membrane induced during the fabrication.

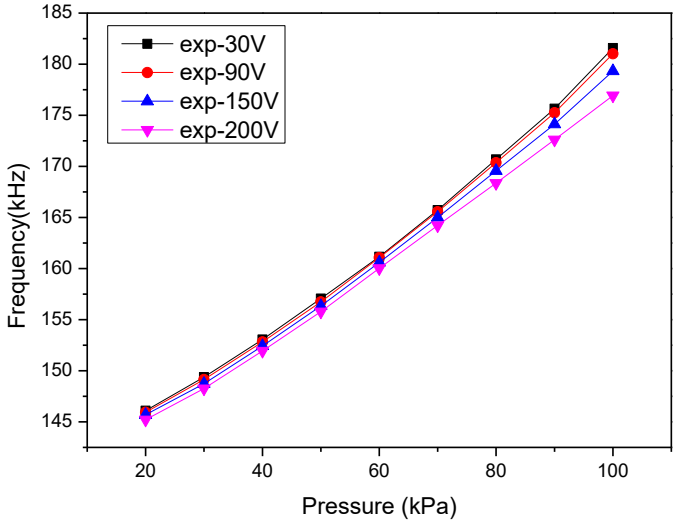

Figure 8 – The resonant frequency variation of the CMUT array

under pressures of 20kPa-101kPa at different voltages

Table 2 – Sensitivity and linearity of pressure curves of cells 2 under different DC bias

DC bias, V	Slope, Hz/kPa	R-square
30	438.14	0.99335
90	434.53	0.9942
150	429.37	0.99607
200	412.42	0.99829

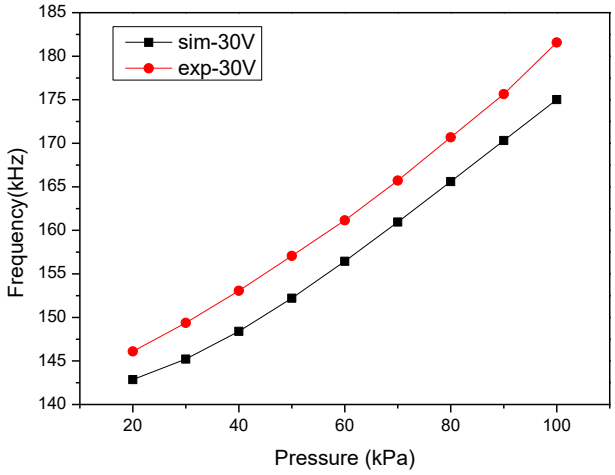

Figure 9 – Comparison of experiment and simulation results of
the resonant frequency variation at 30V, 20kPa-101kPa

5. CONCLUSIONS

A novel method of vacuum pressure monitoring using CMUT is proposed in this paper. The array is designed on the basis of linear relationship between the resonant frequency and the external pressure ranging from 20 kPa-101 kPa. The tendency of frequency shift here is quite different from that in micro-pressure detecting process. With the rise of DC bias, the sensitivity gets lower while the linearity gets higher. The finite element model and the experimental results show a strong agreement. The sensor achieves high detection sensitivity of 438Hz/kPa and R-Square of 0.99335 at DC bias of 30V. The CMUT has simple processing technology, approvable consistency and high yield. It can be used for detection of other pressure ranges only by altering the structure parameters. Integrated circuit will be used to realize portable and miniaturized detection in the future. Therefore, CMUT array has broad application prospects in the field of pressure measurement.

ACKNOWLEDGEMENTS

This work was supported by the National Key Research and Development Program of China (No.2017YFA0205103), the National Natural Science Foundation of China (No.81571766) and the 111 Project of China (No.B07014).

REFERENCES

1. Yang XF, Wang YS, Sun H, and Qing XL. "A flexible ionic liquid-polyurethane sponge capacitive pressure sensor," Sensors and Actuators a-Physical, 1 Jan 2019,vol. 285, p. 67-72.
2. Li C, Xie JB, Cordovilla F, Zhou JQ, Jagdheesh R, and Ocana JL. "Design, fabrication and characterization of an annularly grooved membrane combined with rood beam piezoresistive pressure sensor for low pressure measurements," Sensors and Actuators a-Physical, 15 Aug 2018,vol. 279, p. 525-36.
3. Chou TL, Chu CH, Lin CT, and Chiang KN. "Sensitivity analysis of packaging effect of silicon-based piezoresistive pressure sensor," Sensors and Actuators a-Physical, 21 May 2009, vol. 152, p. 29-38.
4. Joo Y et al., "Silver nanowire-embedded PDMS with a multiscale structure for a highly sensitive and robust flexible pressure sensor," Nanoscale, 2015, vol. 7, p. 6208-15.
5. Zhu BW et al., "Microstructured Graphene Arrays for Highly Sensitive Flexible Tactile Sensors," Small, 24 Sep 2014, vol. 10, p. 3625-31.
6. Luo ZY, Chen DY, Wang JB, Li YN, and Chen J. "A High-Q Resonant Pressure Microsensor with Through-Glass Electrical Interconnections Based on Wafer-Level MEMS Vacuum Packaging," Sensors, Dec 2014, vol. 14, p. 24244-57.
7. Ren S, Yuan WZ, Qiao DY, Deng JJ, and Sun XD. "A Micromachined Pressure Sensor with Integrated Resonator Operating at Atmospheric Pressure," Sensors, Dec 2013, vol. 13, p. 17006-24.
8. Shi XQ et al., "A Resonant Pressure Microsensor Based on Double-Ended Tuning Fork and Electrostatic Excitation/Piezoresistive Detection," Sensors, Aug 2018, vol. 18, 2494, p.1-8.
9. Cheng RJ, Zhao YL, Li C, Tian B, Yu ZL, and Liu KY. "Design and fabrication of a resonant pressure sensor by combination of DETF quartz resonator and silicon diaphragm," Microsystem Technologies-Micro-and Nanosystems-Information Storage and Processing Systems, Mar 2015, vol. 21, p. 631-640,.
10. Du XH, Liu YF, Li AL, Zhou Z, Sun DH, and Wang LY. "Laterally Driven Resonant Pressure Sensor with Etched Silicon Dual Diaphragms and Combined Beams," Sensors, Feb 2016, vol. 16, 158, p: 1-11.
11. Du XH, Wang LY, Li AL, Wang LY, and Sun DH. "High Accuracy Resonant Pressure Sensor with Balanced-Mass DETF Resonator and Twinborn Diaphragms," Journal of Microelectromechanical Systems, Feb 2017, vol. 26, p. 235-45.
12. Cheng RJ, Zhao YL, Li C, Li B, and Zhang Q. "Modelling and characterisation of a micromachined resonant pressure sensor with piezoelectric excitation and sensing," Micro & Nano Letters, Jun 2016, vol. 11, p. 326-31.
13. Chen DY, Li YX, Liu M, and Wang JB. "A Novel Laterally Driven Micromachined Resonant Pressure Sensor," 2010 IEEE Sensors, 2010, p. 1727-1730.
14. Li Z. K. et al., "Capacitive micromachined ultrasonic transducer for ultra-low pressure measurement: Theoretical study," Aip Advances, Dec 2015, vol. 5, no. 12.
15. Li ZK, Zhao LB, Ye ZY, Wang HY, Zhao YL, and Jiang ZD. "Resonant frequency analysis on an electrostatically actuated microplate under uniform hydrostatic pressure," Journal of Physics D-Applied Physics, 15 May 2013, vol. 46, 195108, p:1-7.

16. Yaralioglu GG, Ergun AS, Bayram B, Haeggstrom E, and Khuri-Yakub BT. "Calculation and measurement of electromechanical coupling coefficient of capacitive micromachined ultrasonic transducers," IEEE Transactions on Ultrasonics Ferroelectrics and Frequency Control, Apr 2003, vol. 50, p. 449-56.
17. Samarasekera C, Sun JGW, Zheng Z, and Yeow JTW. "Trapping, separating, and palpating microbead clusters in droplets and flows using capacitive micromachined ultrasonic transducers (CMUTs)," Sensors and Actuators B-Chemical, 10 Dec 2018, vol. 276, p. 481-8.
18. Ergun AS, Huang YL, Zhuang XF, Oralkan O, Yaralioglu GG, and Khuri-Yakub BT, "Capacitive micromachined ultrasonic transducers: Fabrication technology," IEEE Transactions on Ultrasonics Ferroelectrics and Frequency Control, Dec 2005, vol. 52, p. 2242-58.